Supplement

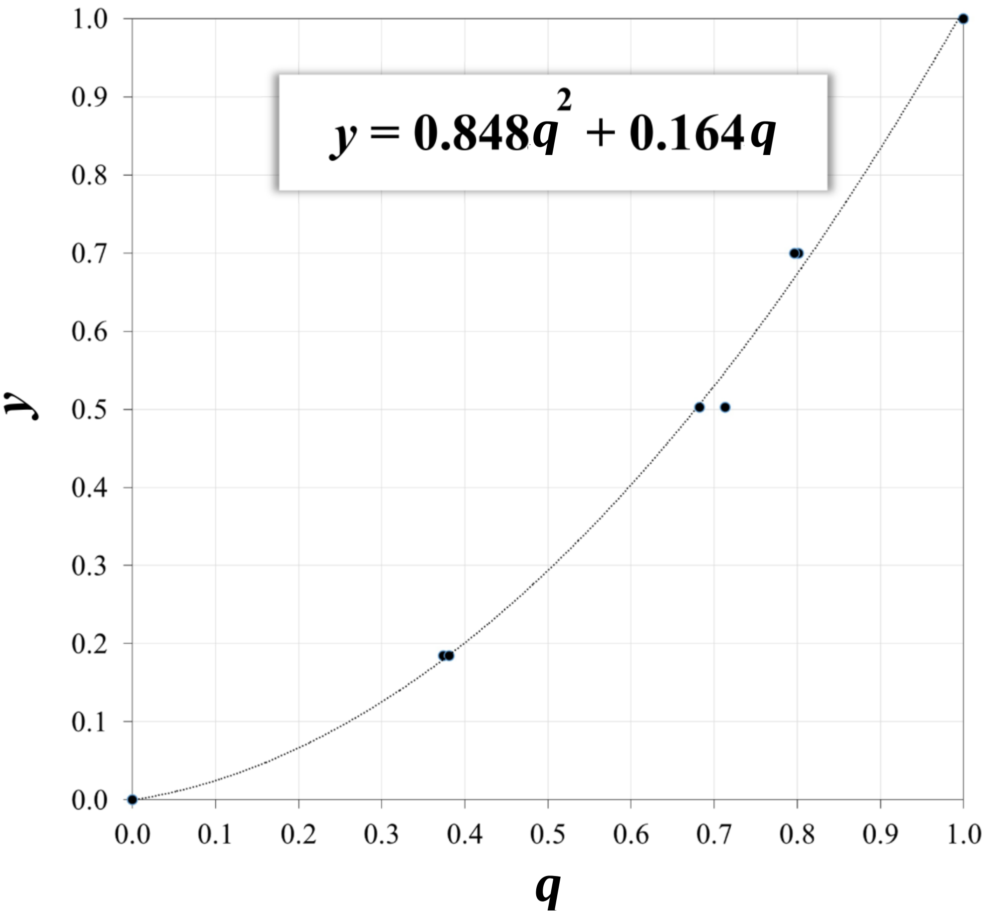

Figure S1. Calibration curve of EDX measurements aimed at the determination of the Fe:Co atomic ratio. The known Fe/(Fe+Co) atomic ratio of standard samples prepared by mixing different amounts of Fe_2O_3 and Co_2O_3 powders are measured along the vertical (y) axis, whereas the corresponding Fe/(Fe+Co) atomic ratio determined via EDX spectroscopy is measured along the horizontal (q) axis. For each of the three standards the results of two successive EDX measurements are depicted on the graph with solid circles. Two additional points were introduced (without corresponding standard measurements) at $(q,y) = (0,0)$ and $(1,1)$ as trivial extreme cases. A second order polynomial with the fixed point of $(q,y) = (0,0)$ was fitted to these data to observe the calibration curve drawn through the points with thin solid line. The equation of the calibration curve is given in the inset. Uncalibrated results of EDX analysis apparently fails to provide the correct Fe/(Fe+Co) ratio, which may be due to the presence of overlapping Fe and Co lines in the X-ray spectrum.

Z. Klencsár, P. Németh, Z. Sándor, T. Horváth, I.E. Sajó, S. Mészáros,
J. Mantilla, J.A.H. Coaquira, V.K. Garg, E. Kuzmann, Gy. Tolnai:
Journal of Alloys and Compounds **674** (2016) 153.
(http://dx.doi.org/10.1016/j.jallcom.2016.03.068)

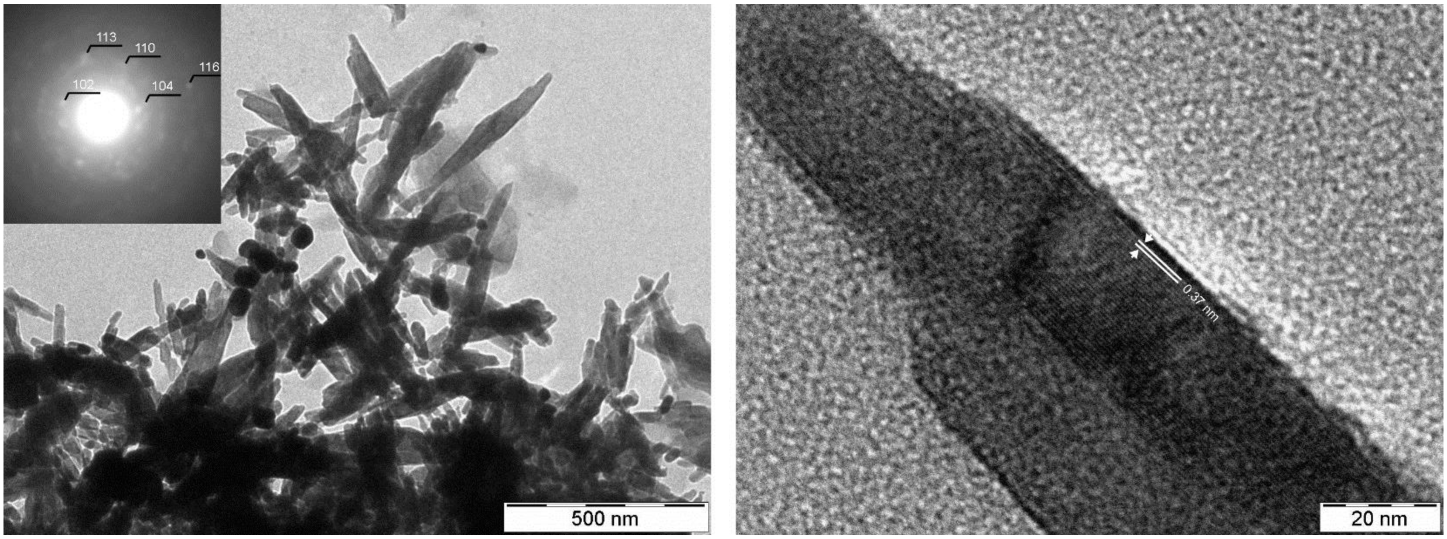

Figure S2. TEM images observed on the heat treated sample DS1, showing the presence of anisometric nanoparticles that can be identified as hematite on the basis of the corresponding SAED pattern (inset).

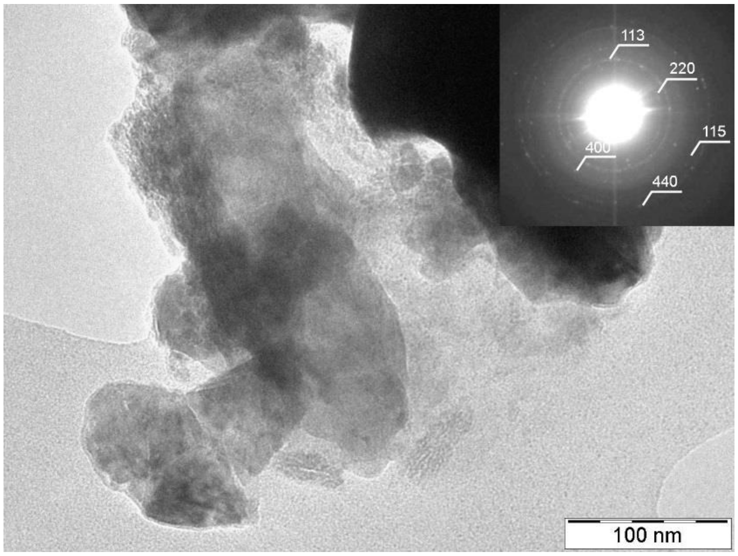

Figure S3. TEM images observed on the heat treated sample DS1, showing the presence of particles with a characteristic size above 100 nm, identified on the basis of the corresponding SAED pattern (inset) as having the spinel structure akin to that of magnetite.

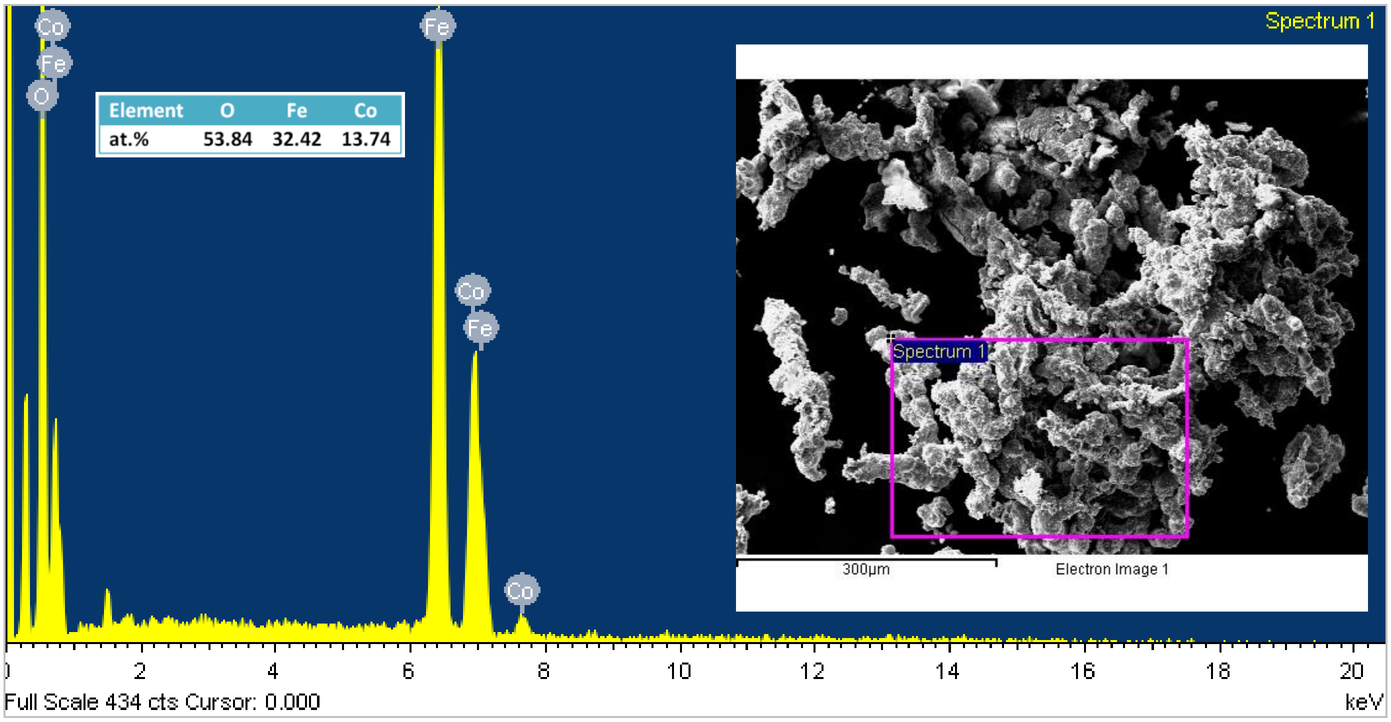

Element	O	Fe	Co
at.%	53.84	32.42	13.74

Figure S4. Typical results of EDX analysis carried out concerning sample DS1. The Fe:Co atomic ratio is reported here to be 70:30. Due to the overlap of several peaks associated with Fe and Co, this result needs to be corrected according to the calibration curve given in Figure S1. See Table 2 for the corrected values.

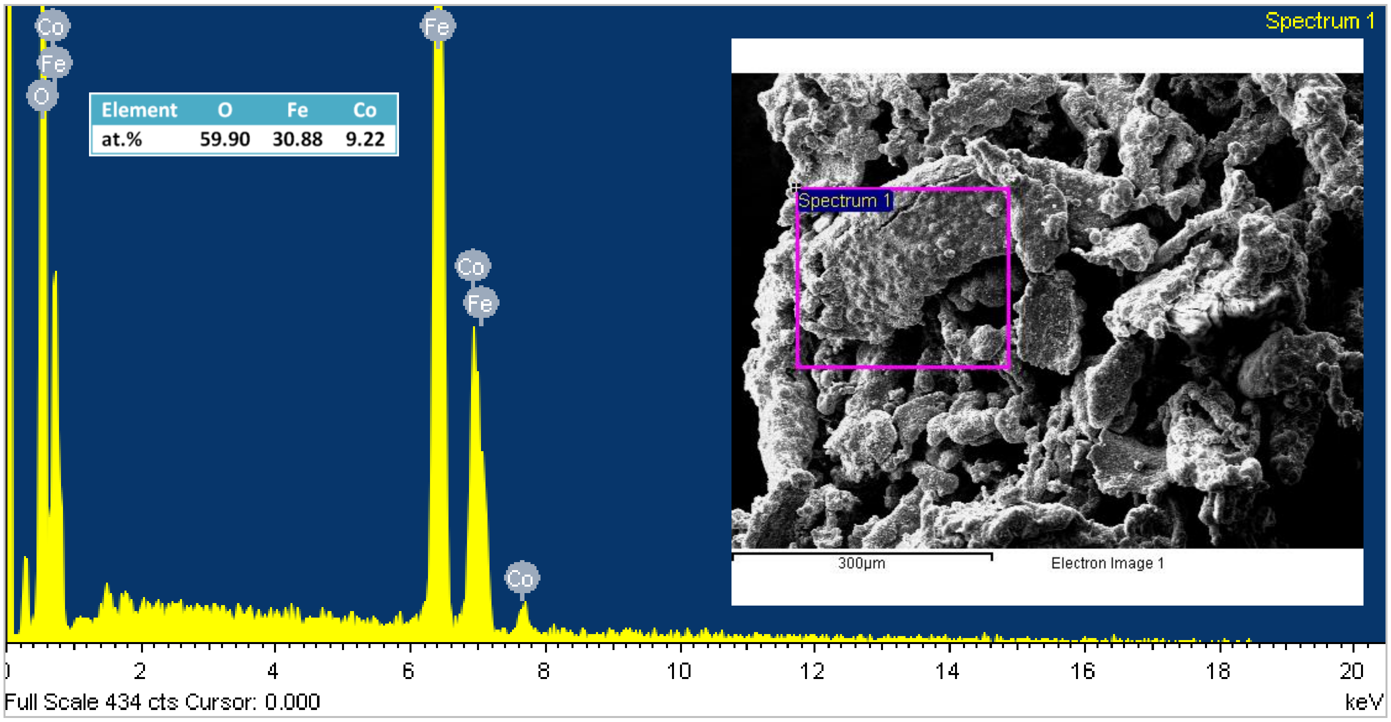

Element	O	Fe	Co
at.%	59.90	30.88	9.22

Figure S5. Typical results of EDX analysis carried out concerning sample DS2. The Fe:Co atomic ratio is reported here to be 77:23. Due to the overlap of several peaks associated with Fe and Co, this result needs to be corrected according to the calibration curve given in Figure S1. See Table 2 for the corrected values.

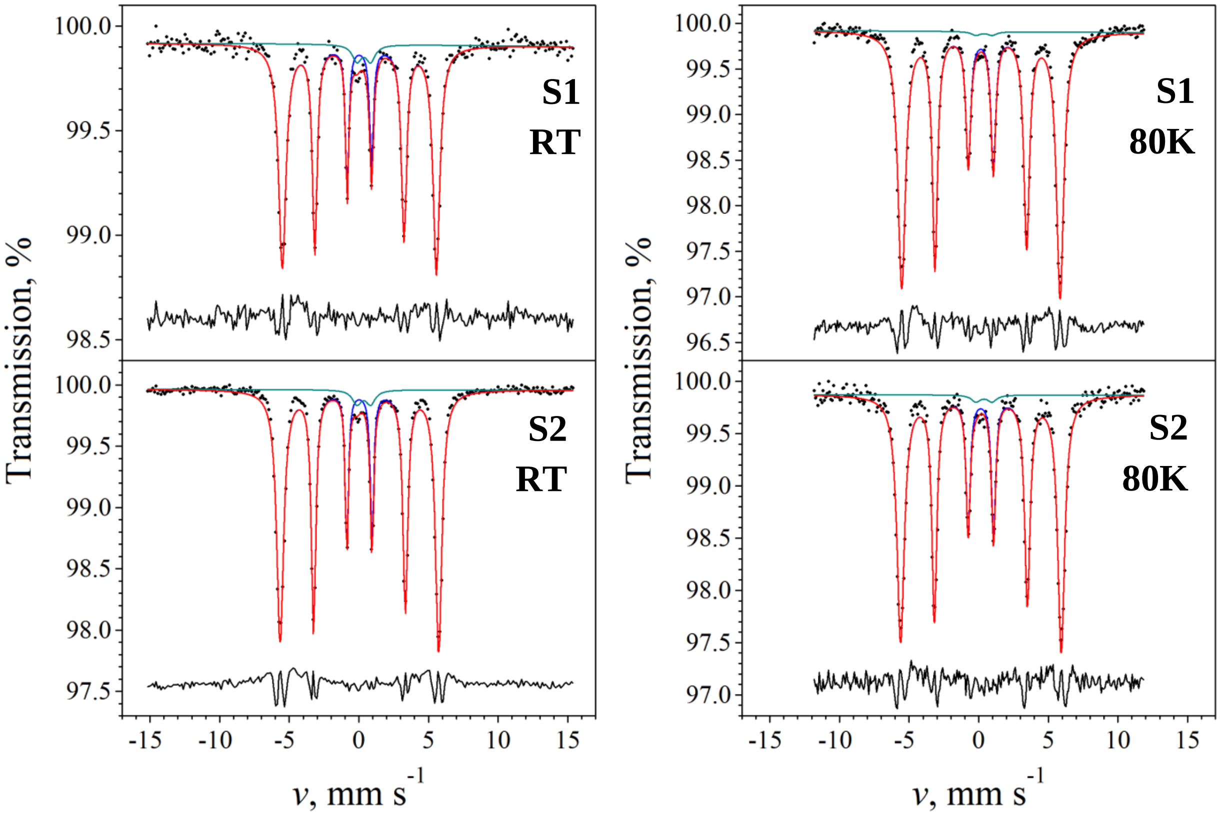

Figure S6. ^{57}Fe Mössbauer spectra (dots) of samples S1 and S2 measured at room temperature ($T \approx 293$ K, left) and at 80 K (right). Solid lines indicate the two subcomponents fitted to the spectra and the corresponding fit envelope. Below the spectra the residual of the fit is displayed. In these fits the magnetic component was accounted for by a single sextet of Lorentzian peaks each of them having independent values for their amplitude and line width. On the basis of the residual it is obvious that the shape of the peaks deviates from Lorentzian, which is due to the presence of atomic disorder in the α-Fe$_x$Co$_{1-x}$ alloy phase, and the associated broadening of the absorption peaks. Compare the residuals shown here with corresponding residuals in Figure S7 and Figure S8.

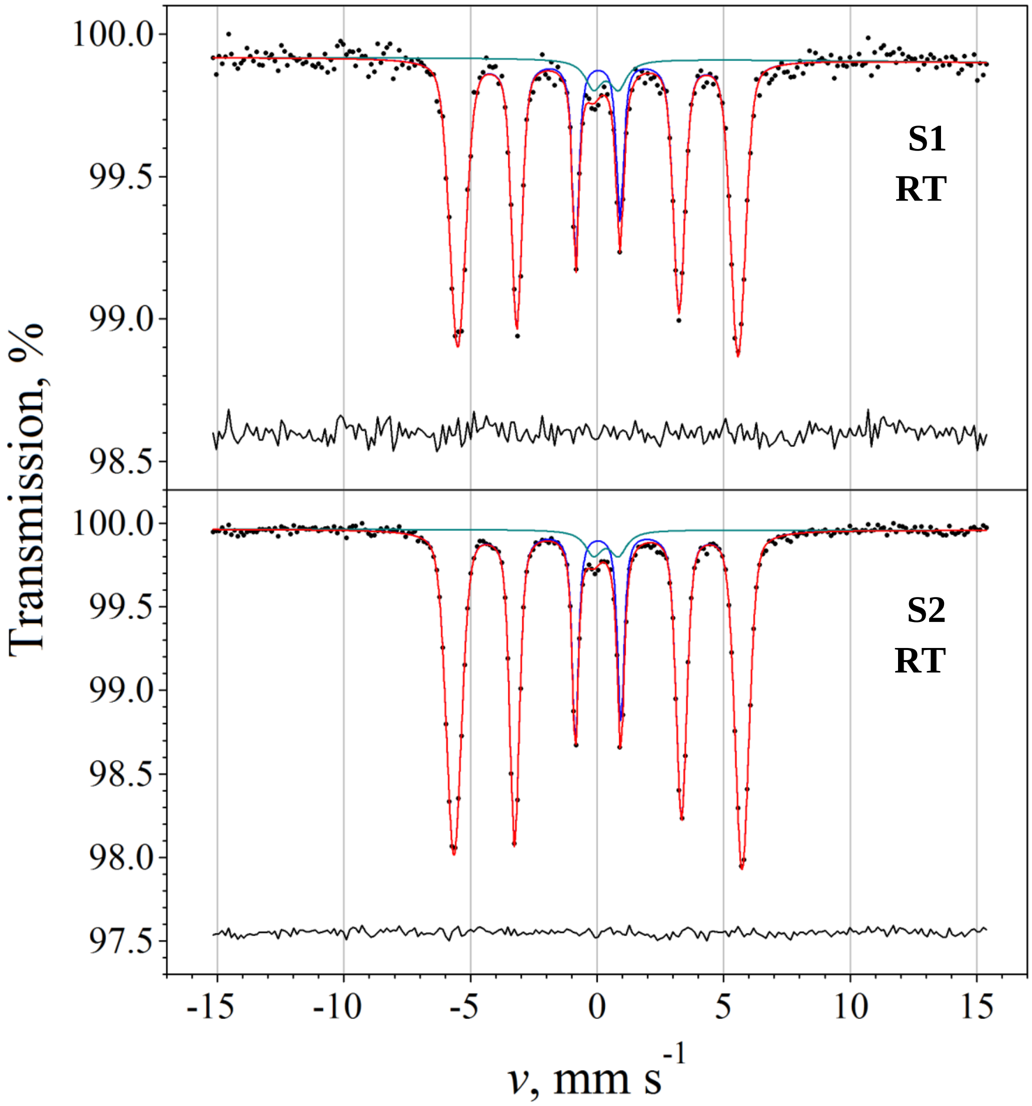

Figure S7. ^{57}Fe Mössbauer spectra (dots) of samples S1 (top) and S2 (bottom) measured at room temperature ($T \approx 293$ K). Solid lines indicate the two subcomponents fitted to the spectra and the corresponding fit envelope. Below the spectra the residual of the fit is displayed. In these fits we aimed at deriving the mean values of the ^{57}Fe B_{hf} hyperfine magnetic field and δ isomer shift parameters characterizing the α-Fe$_x$Co$_{1-x}$ alloy phase, and consequently the magnetic component was accounted for by a single sextet of pseudo-Voigt peaks each of them having independent values for their amplitude and Gaussian broadening, along with a common value of their Lorentzian line width (~ 0.24(1) mm/s). See Table 4 for the resulting fit parameters.

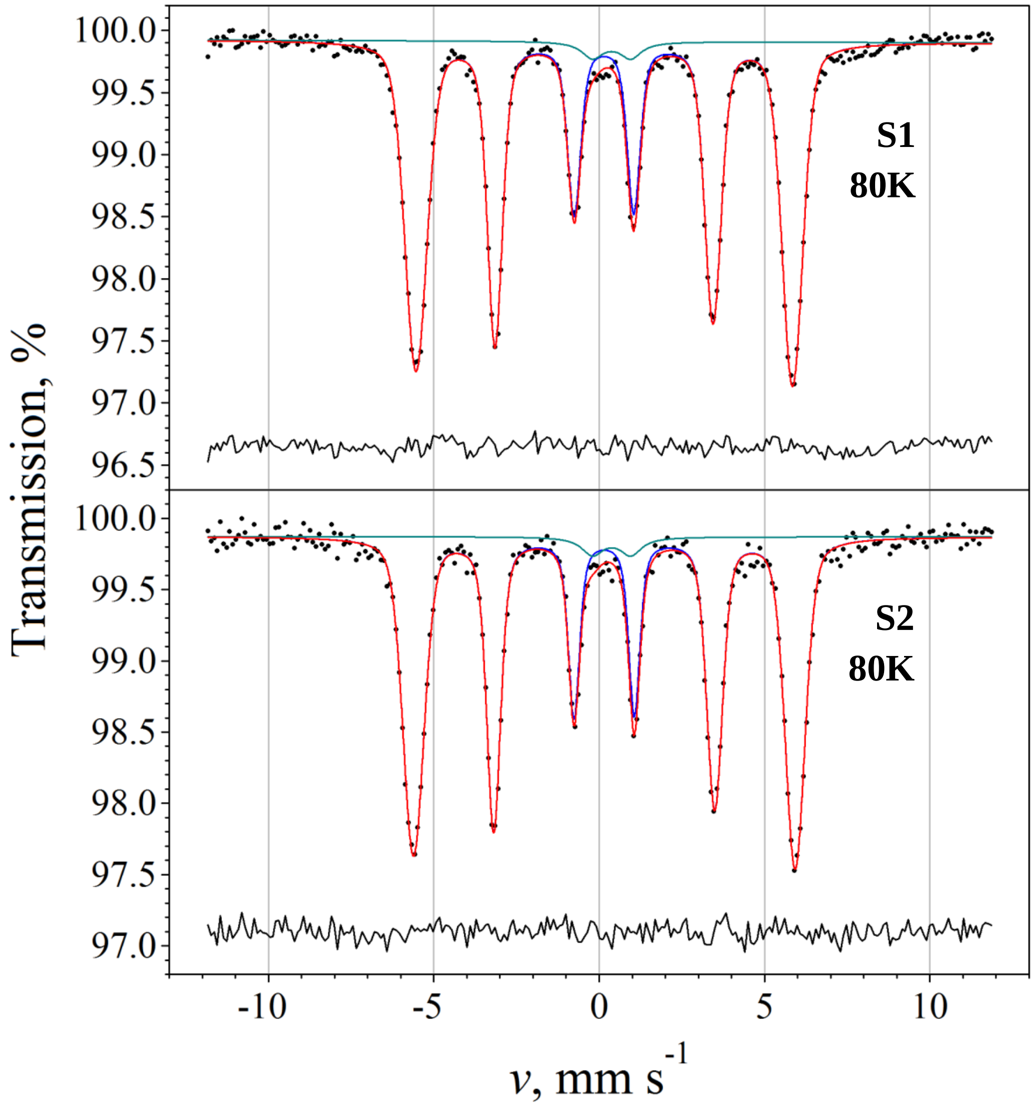

Figure S8. ^{57}Fe Mössbauer spectra (dots) of samples S1 (top) and S2 (bottom) measured at $T \approx 80$ K. Solid lines indicate the two subcomponents fitted to the spectra and the corresponding fit envelope. Below the spectra the residual of the fit is displayed. In these fits we aimed at deriving the mean values of the ^{57}Fe B_{hf} hyperfine magnetic field and δ isomer shift parameters characterizing the α-Fe$_x$Co$_{1-x}$ alloy phase, and consequently the magnetic component was accounted for by a single sextet of pseudo-Voigt peaks each of them having independent values for their amplitude and Gaussian broadening, along with a common value of their Lorentzian line width (~ 0.26(1) mm/s). See Table 4 for the resulting fit parameters.

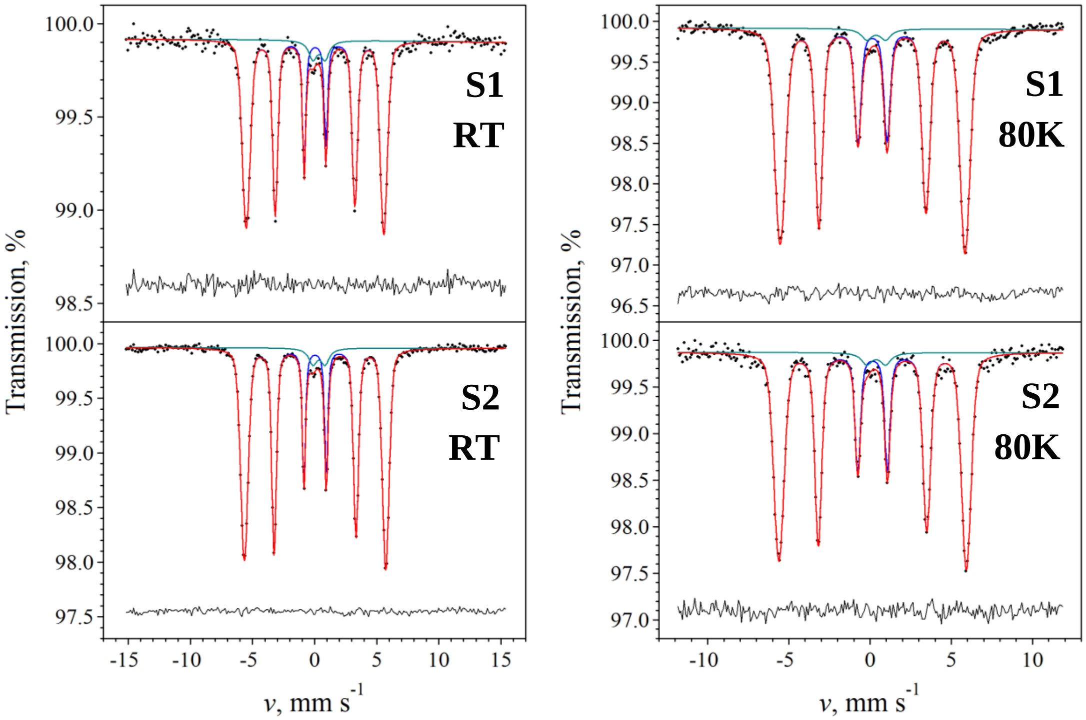

Figure S9. ^{57}Fe Mössbauer spectra (dots) of samples S1 and S2 measured at room temperature ($T \approx 293$ K, left) and at 80 K (right). Solid lines indicate the two subcomponents fitted to the spectra and the corresponding fit envelope. Below the spectra the residual of the fit is displayed. The displayed fits were carried out by modeling the magnetic component with a hyperfine magnetic field distribution derived via the Hesse-Rübartsch method by allowing for a linear correlation between the hyperfine magnetic field (B_{hf}) and the parameters of isomer shift (δ) and double quadrupole shift (2ε). The elementary pattern of the distribution was a sextet with Lorentzian lines of equal line width and relative area ratios 3:2:1:1:2:3 corresponding to a powder sample without texture. The hyperfine field distributions derived in this way are displayed in Figure S10, whereas the corresponding linear correlation parameters are listed in Table S1.

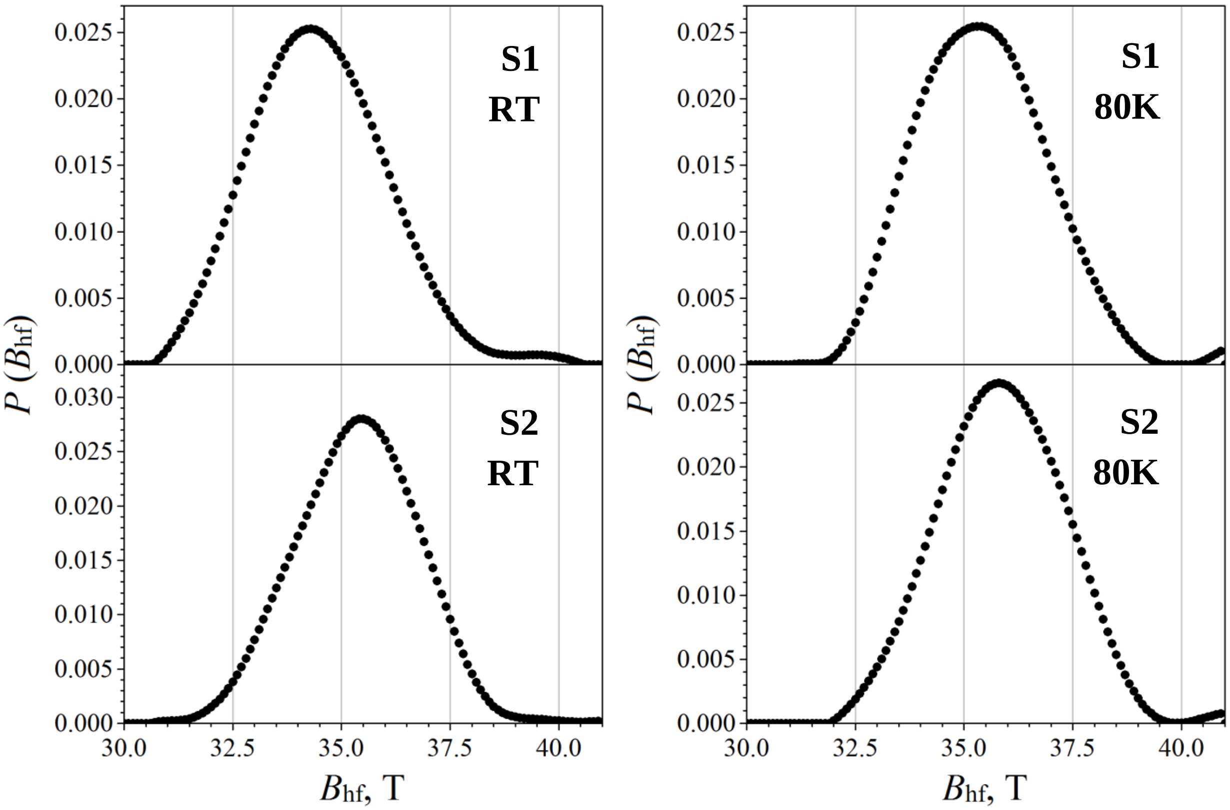

Figure S10. ^{57}Fe hyperfine magnetic field distributions (dots) derived on the basis of ^{57}Fe Mössbauer spectra of α-Fe$_x$Co$_{1-x}$ alloy nanoparticle samples S1 (top) and S2 (bottom) measured at room temperature ($T \approx 293$ K, left) and at 80 K (right). See Figure S9 for the corresponding spectrum fits.

Table S1. Linear correlation parameters between the ^{57}Fe isomer shift, δ, and the hyperfine magnetic field, B_{hf}, and between the double quadrupole shift, 2ε, and B_{hf}, associated with the fits depicted in Figure S9 and Figure S10. The fits were carried out by assuming the same correlation parameter values for samples S1 and S2. Numbers in parentheses denote the standard deviation in the last digit.

	$T \approx 80$ K	$T \approx 293$ K
$\delta(B_{\mathrm{hf}} = 35$ T), mm/s	0.15(1)	0.04(2)
$\mathrm{d}\delta/\mathrm{d}B_{\mathrm{hf}}$, mm/s/T	0.0016(3)	0.0011(6)
$2\varepsilon(B_{\mathrm{hf}} = 35$ T), mm/s	0.01(6)	0.00(4)
$\mathrm{d}(2\varepsilon)/\mathrm{d}B_{\mathrm{hf}}$, mm/s/T	−0.014(2)	−0.015(1)

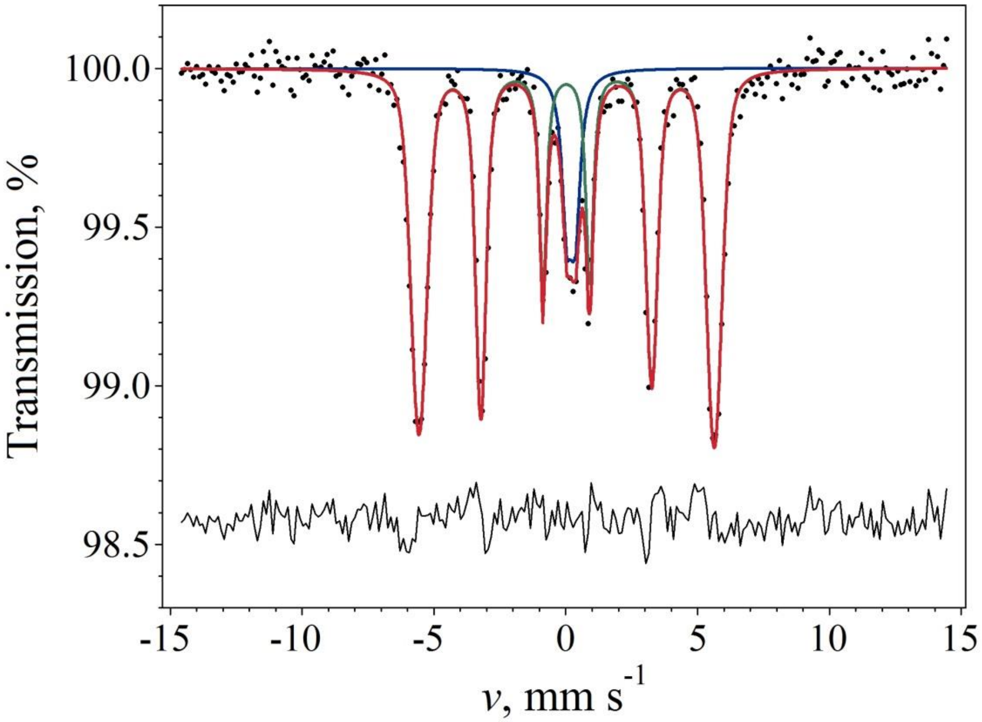

Figure S11. ^{57}Fe Mössbauer spectrum recorded at room temperature ($T \approx 293$ K) on particles of sample S1 that were directly exposed to ambient air for ~ 4.5 months. A quadrupole doublet component with parameters $\delta \approx 0.21(1)$ mm/s, $\Delta \approx 0.32(2)$ mm/s and a relative area fraction of ~ 13% appears in the spectrum referring to the formation of an oxidation product. The doublet can be associated with Fe^{3+} ions situated mainly at the tetrahedral site in a $(Fe,Co)_3O_4$ spinel oxide phase. Majority (~ 87%) of all iron atoms can still be found in the alloy phase contributing to the sextet component.